JOURNAL OF BACTERIOLOGY, Dec. 1984, p. 1067–1073
0021-9193/84/121067-07$02.00/0

Vol. 160, No. 3

Microcinematographic Analysis of Tethered *Leptospira illini*

NYLES W. CHARON,[1]* GLEN R. DAUGHTRY,[1] ROBERT S. McCUSKEY,[2] AND GUNTER N. FRANZ[3]

Departments of Microbiology,[1] Anatomy,[2] and Physiology,[3] West Virginia University, Morgantown, West Virginia 26506

Received 16 July 1984/Accepted 15 September 1984

A model of *Leptospira* motility was recently proposed. One element of the model states that in translating cells the anterior spiral-shaped end gyrates counterclockwise and the posterior hook-shaped end gyrates clockwise. We tested these predictions by analyzing cells tethered to a glass surface. *Leptospira illini* was incubated with antibody-coated latex beads (Ab-beads). These beads adhered to the cells, and subsequently some cells became attached to either the slide or the cover glass via the Ab-beads. As previously reported, these cells rapidly moved back and forth across the surface of the beads. In addition, a general trend was observed: cells tethered to the cover glass rotated clockwise around the Ab-bead; cells tethered to the slide rotated counterclockwise around the Ab-bead. A computer-aided microcinematographic analysis of tethered cells indicated that the direction of rotation of cells around the Ab-bead was a function of both the surface of attachment and the shape of the cell ends. The results can best be explained by assuming that the gyrating ends interact with the glass surface to cause rotation around the Ab-beads. The analysis obtained indicates that the hook- and spiral-shaped ends rotate in the directions predicted by the model. In addition, the tethered cell assay permitted detection of rapid, coordinated reversals of the cell ends, e.g., cells rapidly switched from a hook-spiral configuration to a spiral-hook configuration. These results suggest the existance of a mechanism which coordinates the shape of the cell ends of *L. illini*.

Leptospira is a spirochete with a unique structure and mode of motility. These right-handed (7, 15, 17, 34), helically shaped cells have a diameter of approximately 0.12 μm and a length of 10 to 20 μm. A membrane sheath is outermost, and within this sheath are two periplasmic flagella (PF; also referred to as axial filaments, endoflagella [6, 11, 15]). Each PF is subterminally attached to opposite ends of the cell cylinder; the PFs generally do not overlap (4, 5, 12). Cells undergoing translational motion have a spiral-shaped anterior end and a hook-shaped posterior end (Fig. 1c) (2, 6, 9, 14, 25). Nontranslating cells have either both ends spiral shaped or both ends hook shaped (Fig. 1a and b) (2, 6, 14). Cells can change from one form to the other.

We recently proposed a model to explain how these spirochetes swim (2). This model is based on an analysis of motility mutants of *Leptospira illini* which have altered PFs (5). The model states that the PFs propel the organisms by rotation in a manner analogous to flagella rotation in rod-shaped bacteria (29). In addition, the shapes of the cell ends are determined by the shape of the PFs. Rotation of the PFs in one direction causes that end to be spiral shaped, and rotation in the opposite direction results in that end being hook shaped.

Two modes of motility have been proposed (2). First, rotation of the anterior PF causes the anterior end of the cell to gyrate (i.e., to bend in a circular motion and not necessarily to rotate, in analogy to the laterally bending rubber tube with an internally rotating bent wire as diagrammed by Taylor [32]). This gyration generates a backward-moving spiral wave. It is this spiral wave that propels the cell in a low-viscosity medium. The other mode is due to the cell rolling around the PF. It is this motion which allows the spirochetes to swim through gel-like media such as methylcellulose (3) without slippage. Both motions occur together: the PF rotates in one direction, and the cell cylinder rolls in the opposite direction.

* Corresponding author.

The different forms of motile cells (Fig. 1) can be explained by the model (2). As viewed from the center of the cell toward the ends, nontranslating cells have both PFs rotating in the same direction, and translating cells have their PFs rotating in opposite directions. The model predicts that given cells with right-handed helical bodies, translating cells have the anterior spiral-shaped end gyrating counterclockwise (CCW) and the posterior hook-shaped end gyrating clockwise (CW) (2, 7). We now present evidence that the ends do indeed gyrate in these directions. The approach we used was to track the motions of cells with both ends spiral shaped and cells with both ends hook shaped. These cells were tethered to a glass surface via antibody-coated latex beads (Ab-beads) (8). In the process of doing these experiments, we also found that the cells could coordinate reversals of the cell ends as is found in *Spirillum* sp. (18, 24).

(This work was presented in part at the annual meeting of the American Society for Microbiology [N. Charon, G. Daughtry, R. McCuskey, and G. Franz, Abstr. Annu. Meet. Am. Soc. Microbiol. 1983, I71, p. 151].)

MATERIALS AND METHODS

Organism and culture conditions. *L. illini* 3055 was obtained from R. C. Johnson, University of Minnesota, Minneapolis. Cells were maintained in the Tween 80–bovine serum albumin (Scientific Protein Laboratories, Waunakee, Wis.) complete medium described by Ellinghausen and McCullough and modified by Johnson and Harris (16) (EMJH medium). Cultures were maintained at 30°C on a rotary environmental shaker, and cell growth was monitored by nephelometry with a Coleman model 7 nephelometer (16).

Tethering cells via Ab-beads. The conditions for tethering cells to glass surfaces via Ab-beads are similar to those previously described (8). To prepare Ab-beads, 1 ml of rabbit anti-*L. illini* immunoglobulin (65 to 650 μg of protein) was mixed with 1 ml of latex beads (radius 0.13 μm; Duke Scientific, Palo Alto, Calif.). The latex bead suspension was prepared by diluting 0.1 ml of beads (2×10^{10} to 2×10^{11} per ml) with 4.9 ml of glycine-saline buffer (G-buffer), pH 9.6

(30). After incubation of the Ab-bead suspension for 3 h at 23°C, 12 ml of G-buffer containing 0.5% bovine serum albumin was added to the tube. The Ab-bead suspension was gently layered onto a 4-ml 45% (wt/vol) sucrose cushion and centrifuged for 30 min at 42,000 × *g* in a Beckman SW27.1 rotor at 20°C. The Ab-beads banded at the G-buffer–sucrose interface and were obtained by piercing the bottom of the tube and collecting the fractions containing the Ab-beads. The Ab-beads were stored in a final volume between 0.5 and 2 ml in G-buffer at 4°C. To attach Ab-beads to cells, logarithmic-phase cells were diluted to 10^8 cells per ml in EMJH basal medium supplemented with 0.5% bovine serum albumin and 0.8% NaCl. A 40-μl sample of these cells was mixed with 5 to 15 μl of Ab-beads for 2 min at 23°C. The amount of Ab-bead suspension was adjusted to achieve at least 50% of the cells with attached Ab-beads. Approximately 20 μl of this suspension was placed onto a precleaned slide and sealed with a cover glass (22 by 40 mm) with silicone grease along its edges. Approximately 1 to 5% of the cells with attached Ab-beads spontaneously became tethered to the cover glass and slide in these preparations.

Microcinematography. Tethered cells were studied under dark-field illumination with a modified Leitz Panphot microscope equipped with an XBO-150 Xenon lamp (23), dark-field condenser, and 90× oil immersion objective and appropriate oculars. A yellow barrier filter having a 50% cutoff at 530 nm (Fish Schurman, New Rochelle, N.Y.) was placed in front of the light source (8, 21). The microscopic images were recorded on videotape with a silicon vidicon television system in combination with a 1-in. (2.5-cm) video tape recorder. Permanent records were made by either transferring images onto 0.75-in. (1.9-cm) video cassettes or by kine-recording at 30 frames per s from a 17-in. (43-cm) monitor with a 16-mm Arriflex 16-S motion picture camera equipped with a special motor to synchronize the framing of the video and photographic images (23). Cell lengths were determined by using similarly recorded images of a stage micrometer. With the optical system used, the recorded micrometer images were found not to be reversed from left to right.

Analysis of tethered cells. Four parameters were recorded at 0.5-s intervals (15 frames on the 16-mm film) on a stop-motion analyzer. The data were entered into a PDP-11/23 computer to calculate the various cellular movements as a function of time. A Tektronix model 4662 digital plotter was used to display the results. The parameters recorded included the following. (i) The shape of each end of the cell, i.e., were they hook or spiral shaped? The ends were arbitrarily assigned the designation end A or end B. A double line in the figures refers to that end being hook shaped and a single line refers to that end being spiral shaped. (ii) The relative position of the Ab-bead as determined by measuring the distance from the Ab-bead to one of the cell ends. (iii) The angular position of the cell, using a coordinate axis with end A serving as the reference. Rapid transitions from 360 to 0° in the position diagrams represent the beginning of new rotational cycles as the cell crosses the 0°/360° reference line. Thus, the rapid transitions are artifacts of the plotting method. (iv) The angular velocity around the Ab-bead as expressed in degrees per second. The angular velocity was determined by the digital low-pass differentiation procedure of Usui and Amidror (33). CCW rotation is represented by a positive angular velocity (positive slope of the position trace) and CW rotation as a negative angular velocity (negative slope of the position trace).

RESULTS

Tethered cell assay. Latex beads coated with antibody directed to *L. illini* (Ab-beads) were attached to motile cells. Some of these cells became attached to the cover glass or slide via the Ab-beads. As we previously reported, these tethered cells swam back and forth across the surface of the Ab-bead (8). For example, when cells changed from a spiral-spiral configuration to a hook-spiral configuration, the Ab-bead was displaced rapidly to the hook-shaped end without slippage, i.e., the cells literally screwed their way along the Ab-bead (Fig. 2). We interpret this phenomenon as follows (8). The Ab-bead is attached to an antigen of the outer sheath. This antigen is dragged laterally through the sheath to the back end due to the forward motion of the cell and the opposite retarding force acting on the immobilized Ab-bead.

Rotation around fixed Ab-beads. A general trend was observed when we were analyzing the tethered cells. These cells occasionally aligned themselves parallel to the slide or cover glass. The aligned cells were found to rotate CW around the Ab-bead if the Ab-bead was attached to the coverglass and CCW if the Ab-bead was attached to the slide (Fig. 2). The rotational motion was most apparent when the cells were in the spiral-spiral configuration. In contrast to tethered cells, free-swimming cells did not rotate around an attached Ab-bead.

To better understand the rotational motions of tethered cells, cells were videotaped, and the images were transferred onto 16-mm film. Four parameters of tethered cells were recorded every 0.5 s, and these data were analyzed with the aid of a computer. These parameters included the shape of each of the cell ends, the position of the Ab-bead on the cell, the angular position of the cell as determined with a coordinate axis, and the angular velocity of the cell as it rotated around the fixed Ab-bead.

Cell tethered to the cover glass. As can be seen for the cell attached to the cover glass (Fig. 3), the cell rotated CW around the Ab-bead during an entire minute. The shape of end A went from spiral to hook to spiral. End B was spiral shaped over the entire minute. The cell was in the spiral-spiral configuration for the first 43 s and the last 7 s. The cell in this configuration rapidly rotated around the Ab-bead. It did not roll around its longitudinal axis, as the cell helices were clearly discernible. In the 43-s interval, the Ab-bead was first in the middle of the cell and then became displaced toward end B. At the same time, the angular velocity slowed from 100°/s to 50°/s. When end A formed a hook, the Ab-bead was immediately displaced to that end. This rapid displacement occurred without slippage, i.e., the cell efficiently screwed forward until the Ab-bead reached the back end. The hook-shaped end did not rotate when it was adjacent to the bead and appeared fixed. When the cell was in the hook-spiral configuration, the cell slowed down to angular velocities between 5 and 25°/s.

Cell tethered to the slide. Figure 4 shows an analysis of a cell tethered to a slide. As opposed to the cell attached to the cover glass described above, there were many alternations of both ends in forming hook- and spiral-shaped ends. Ends A and B alternated eight times each. Eight of these 16 reversals were coordinated, i.e., when end A changed from spiral to hook shaped, end B concomitantly changed from hook to spiral shaped. These coordinated reversals, depicted by the arrows, occurred within 0.5 s. In one of these coordinated reversals (not shown in Fig. 4), the resolution in the recorded images was sufficient to detect a reversal within

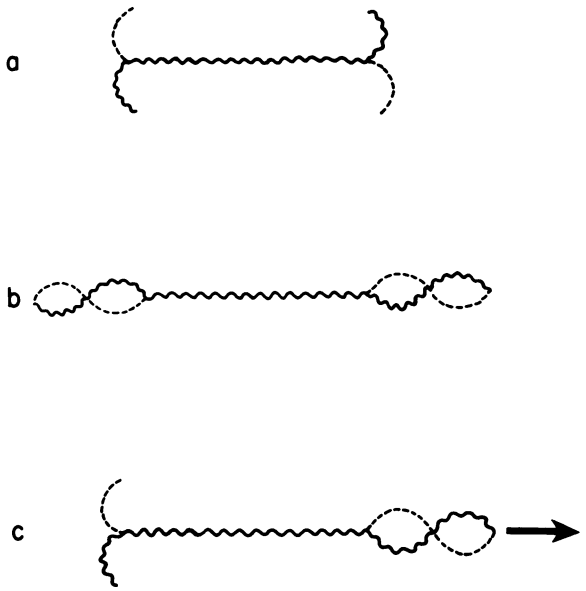

FIG. 1. Movement of *L. illini* in liquid media. (a) and (b) are nontranslational forms and are referred to as the hook-hook (a) or spiral-spiral (b) configurations. Translating cells (c) are in the hook-spiral (or spiral-hook) configuration. The arrow points toward the direction of swimming. Modified from Berg et al. (2).

two frames of the 16-mm film, or 0.06 s. The cell attached to the slide was similar in most respects to the cell attached to the cover glass except that it rotated CCW around the Ab-bead. Thus, the Ab-bead was displaced to the hook-shaped end as soon as the hook was formed, and the cell increased its angular velocity in two of the three spiral-spiral intervals.

Analysis of many cells. A number of cells were examined with respect to their direction of rotation and the shape of the cell ends. We monitored these variables when the cells formed spiral-spiral and hook-hook configurations. We also monitored whether a given cell showed coordinated reversals. We did not monitor the direction of cell rotation in the hook-spiral configuration, as in many of these events the spiral-shaped end went out of the plane of focus. Of the 118 spiral-spiral events in the 21 cells analyzed, 115 were similar to the spiral-spiral events in Fig. 3 and 4 (Table 1). Thus, in all but a few of the events in the spiral-spiral configuration, cells rotated CW around the Ab-bead when tethered to the cover glass and CCW when tethered to the slide. In those few instances when the cell did not rotate, the cells appeared stuck to the glass itself.

No rolling of the cell cylinder was detected when the cells were in the spiral-spiral configuration. This lack of rolling is most evident on cells videotaped for several minutes. The gyrations of the cell ends gradually slowed down and thus became clearly visible. There was no concomitant rolling of the cell cylinder. In addition, the rate of rotation around the Ab-bead decreased as the gyration of the cell ends slowed; the cell ends stopped gyrating as the cell stopped rotating around the Ab-bead.

Only four hook-hook events were observed; the cells in these cases rotated in a direction opposite to that in the spiral-spiral configuration, i.e., they went CW when tethered to the slide and CCW when tethered to the cover glass. As with cells in the spiral-spiral configuration, no rolling of the cell cylinder was detected in cells in the hook-hook configuration. One hook-hook event is depicted in Fig. 5 for a cell tethered to the slide. As can be seen, the cell rotated CCW when in the spiral-spiral configuration. When the cell shifted to a hook-hook configuration, the Ab-bead remained in the center of the cell, but the cell reversed its direction from CCW to CW, i.e., it went from 90 to 0°, and the angular velocity became negative.

The cells were monitored for coordinated reversals of the shape of the cell ends. Two patterns were observed. The first pattern had cells with one end locked into the spiral shape, while the other end alternated from hook to spiral shape as in Fig. 3. Approximately two-thirds of the cells had this pattern. The other pattern was similar to that of the cell shown in Fig. 4, whereby the change of shape of the cell ends were often coordinated.

DISCUSSION

Our initial goal of attaching Ab-beads to swimming cells was aimed at monitoring the direction of roll of translating cells (2, 8). In the process of doing these experiments, we first observed that Ab-beads were displaced to the back end of swimming cells (8). Subsequent observations revealed that cells rotated around fixed Ab-beads when tethered to a surface by these beads.

The results obtained show that *L. illini* differs from other bacteria which rotate around a fixed point when tethered to a surface. In *Escherichia coli* (29), *Salmonella typhimurium* (31), *Streptococcus* sp. strain V4051 (22), and *Bacillus subtilis* (28), cells rotate about a flagellum which is stuck to the glass surface. The structure in spirochetes which is analogous to flagella is the PF. The PFs have been shown to be involved in the motility of a number of spirochetes including *L. illini* (5), *Spirochaeta aurantia* (26), and *Treponema phagedenis* (R. J. Limberger and N. W. Charon, Abstr. Annu. Meet. Am. Soc. Microbiol. 1984, I119, p. 141; manuscript in preparation). Because the PFs are internal (6, 11, 15) and because the Ab-beads attach to the outer surface of *L. illini* (8; unpublished data), it is unlikely that the Ab-beads in our experiments are attaching to the PFs. In addition, our previous results (8) and the results presented here suggest that the Ab-bead motions on a cell are a consequence of cell movement. This passive motion of the Ab-beads differs from the active motion of latex beads attached to gliding bacteria (19, 27). For example, latex beads attached to gliding bacteria move in many different directions when attached to a free cell (19, 27), whereas in *Leptospira* sp. the Ab-beads are displaced to the back end due to viscous drag (8).

An analysis of tethered cells in the spiral-spiral configuration indicates that the cells interact with the adjacent glass which leads to rotation around the Ab-bead. Freely swimming spiral-spiral-shaped cells do not rotate around attached Ab-beads. Evidently, tethering of the cells to a surface is necessary for the rotation. In addition, the dichotomous relationship of CW versus CCW rotation as a function of surface of attachment further supports this conclusion.

We attribute the rotation around an Ab-bead of cells in the spiral-spiral configuration to the gyrations of the cell ends. Thus, the only discernible motion of tethered spiral-spiral-shaped cells, as clearly visible when the rate of rotation around the Ab-bead decreases, is the gyration of the cell ends. In addition, the rate of rotation around the Ab-bead is reflected in the motion at the spiral-shaped ends. We observed that as the gyrations of the spiral-shaped ends slow down and finally stop, the rate of rotation around an Ab-bead concomitantly decreases and stops.

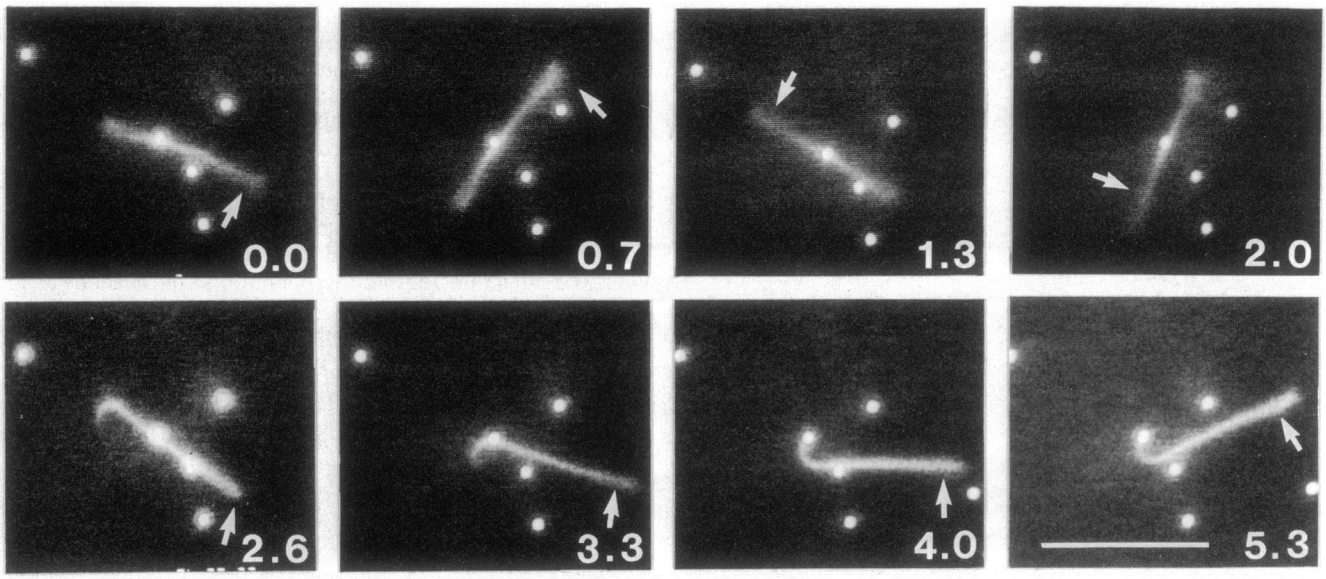

FIG. 2. Selected sequential frames from a 16-mm film of a cell tethered to a slide illustrating CCW rotation around an Ab-bead and spiral- and hook-shaped ends. The bar represents 10 μm, and the numbers refer to time in seconds. The arrow points to one end of the cell as it rotates around the Ab-bead. A hook-shaped end is first evident in the frame marked 2.6 seconds. The Ab-bead is rapidly displaced to that end.

The direction of rotation of cells in the spiral-spiral configuration as a function of whether the cell is attached to the cover glass or to the slide indicates that the spiral-shaped end gyrates CCW. Figure 6 represents a cell in the spiral-spiral configuration tethered to a top surface, such as a slide, via an Ab-bead. As ends A and B gyrate CCW (as viewed from the Ab-bead toward the cell ends) and interact with the surface, the cell rotates CCW around the Ab-bead as viewed

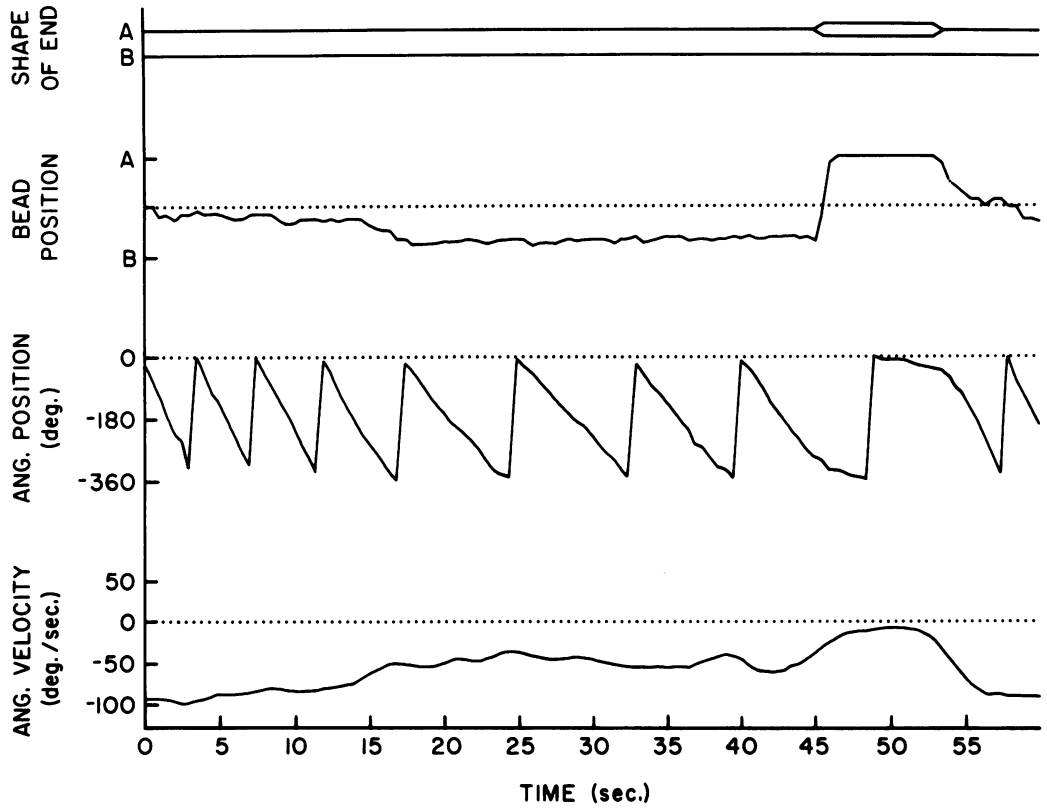

FIG. 3. Computer analysis of a cell (cell length, 11 μm) tethered to a cover glass. A and B represent ends designated A and B. The double horizontal line in the top of the diagram represents a hook-shaped end; the single line represents a spiral-shaped end. CW rotation is represented by a negative angular velocity.

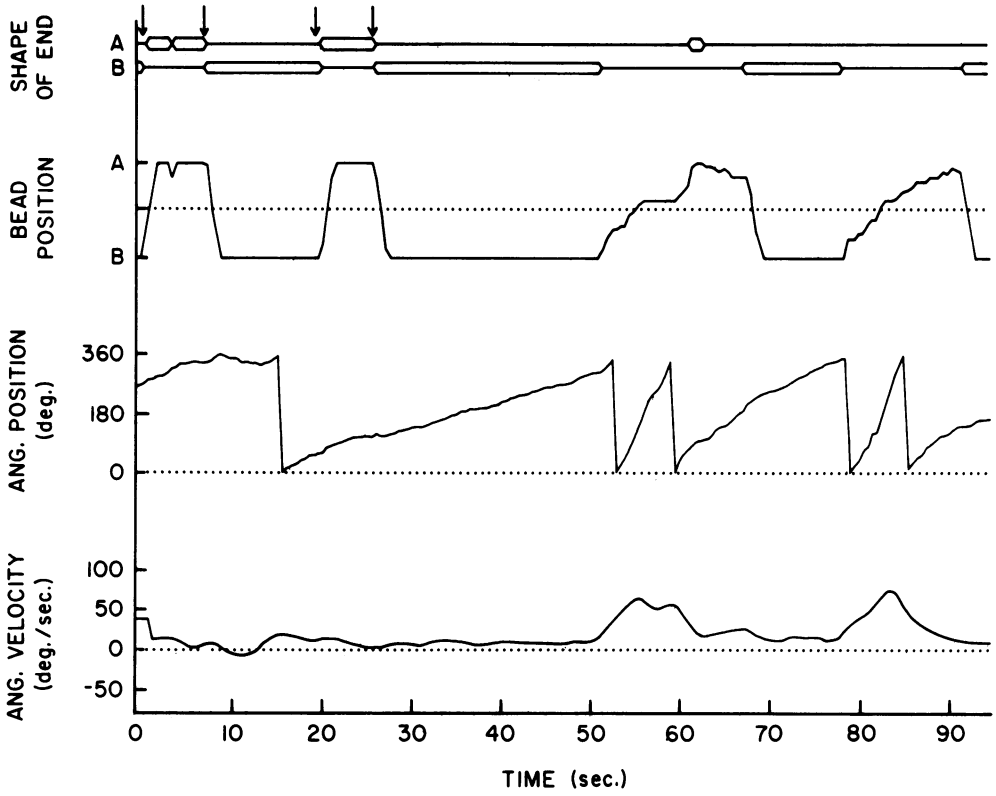

FIG. 4. Computer analysis of a cell (cell length, 14 μm) tethered to a slide. CCW rotation is represented by a positive angular velocity. The arrows point to coordinated reversals of the cell ends. See the legend to Fig. 3 for details.

from above. The opposing forces generating the backward-moving spiral waves cancel, the cell does not roll, and the Ab-bead tends to be near the central part of the cell. On the other hand, if the cell is tethered to a bottom surface such as a cover glass, the gyrating spiral-shaped ends interact with the cover glass and rotate the cell CW as viewed from above. Thus, CCW rotation around an Ab-bead of a cell tethered to a slide and CW rotation of a cell tethered to a cover-glass are reasonably explained by a CCW gyration of the spiral-shaped ends which interact with the appropriate glass surfaces.

We do not know the precise nature of the interaction with the spiral-shaped ends and the glass surface. It may be that the spiral-shaped end, instead of slipping, interacts with the glass itself to carry the cell on a CCW or CW arc around the surface. On the other hand, experiments by Berg (1) showed that viscous drag increases as the cell approaches the surface of the glass. This, too, would reduce the slip of the gyrating end along the glass surface. We favor this latter hypothesis, as the cell body rarely sticks to the glass as it smoothly rotates around the Ab-bead. In addition, others have attributed unusual swimming behavior of bacteria near a glass surface to the increase in viscous drag, e.g., *E. coli* cells swim in CW spirals along a slide and CCW spirals under a cover glass (H. Berg, personal communication).

An analysis of the cells in the rarely occurring hook-hook configuration indicates that the hook-shaped ends gyrate CW. As with cells in the spiral-spiral configuration, the cell cylinder in the hook-hook configuration does not roll. Because cells in the hook-hook configuration rotate around the Ab-beads in the opposite direction from cells in the spiral-spiral configuration, we conclude that hook-shaped ends gyrate CW. In sum, the direction of rotation of both the spiral- and hook-shaped ends supports the proposed model of motility (2).

The greater angular velocity of cells in the spiral-spiral configuration relative to cells in the hook-spiral configuration is probably the result of two factors. First, because our results suggest that both ends of cells in the spiral-spiral configuration gyrate CCW, the ends would act synergically to rotate the cell around the fixed Ab-bead. Cells in the hook-spiral configuration would be gyrating their only free end CCW. Second, the spiral-shaped end of cells in the hook-spiral configuration often goes out of the plane parallel to the surface. As a result, this end would not readily interact with the surface and cause the cell to rapidly rotate around the Ab-bead.

TABLE 1. Direction of rotation of cells tethered to the cover glass or slide

Direction of rotation	Rotation and cell configuration[a]			
	Tethered to cover glass (n = 8)		Tethered to slide (n = 13)	
	Spiral-spiral	Hook-hook	Spiral-spiral	Hook-hook
CW	64/65	0	0	2/2
CCW	0	2/2	51/53	0
No rotation	1/65	0	2/53	0

[a] Results are expressed as the number of events of cells rotating in a given direction/total number events in a given configuration. Results are from cells observed between 26 s and 13.8 min. The mean (± standard error of the mean) interval of a spiral-spiral event varied from cell to cell and ranged from 2.5 ± 0.9 s to 31.7 ± 12.6 s. The mean interval of a hook-hook event was 2.0 ± 0.25 s.

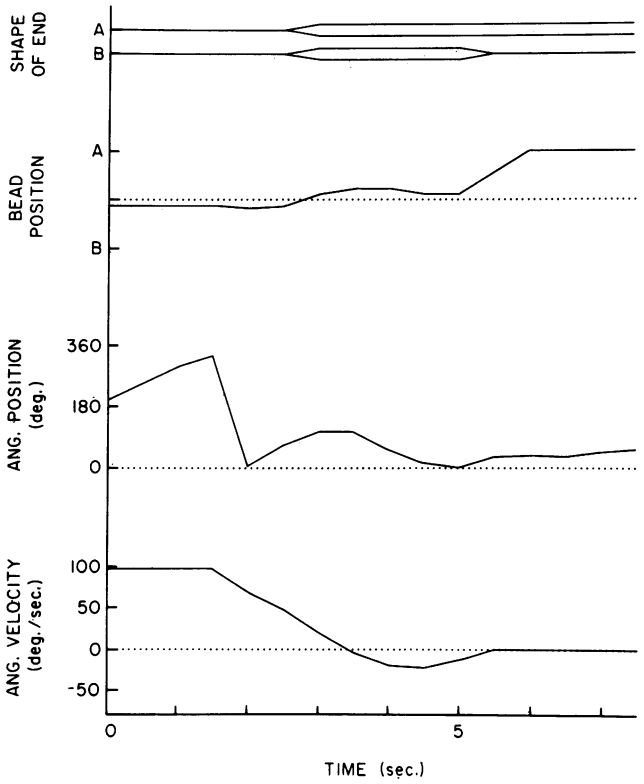

FIG. 5. Computer analysis of a cell (cell length, 13 μm) tethered to a slide illustrating the opposite direction of rotation of a cell in the hook-hook versus the spiral-spiral configuration. See the legend to Fig. 3 for details.

The tethered cell assay permitted us to detect coordinate reversal of the cell ends. One of these coordinate reversals occurred within 0.06 s, which is identical to the coordinate reversals of the flagellar fascicles of *Spirillum volutans* (18). Rapid reversals in direction have also been noted in *Spirochaeta aurantia* (E. P. Greenberg, personal communication). In *Spirochaeta aurantia*, chemotaxis involves an electrical potential (10) and presumably flagella reversal. As with *Spirillum* sp. (24), not all the events in *L. illini* were coordinated in those cells positive for coordination. However, because many were coordinated, as were 8 of 16 events in the cell diagrammed in Fig. 4, the possibility is unlikely that these events occur by chance alone. As suggested by Metzner for *Spirillum* sp. (24), there apparently is an overriding mechanism within the cell which can, but not always, function to coordinate reversal of the cell ends.

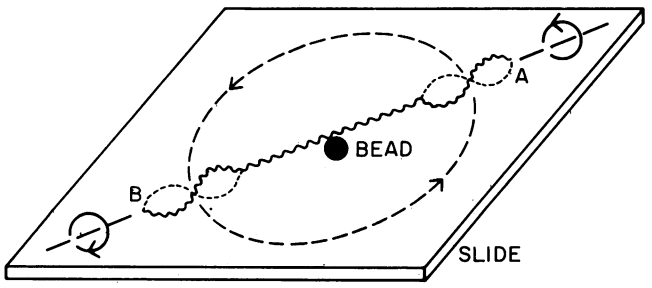

FIG. 6. Model diagram of a cell in the spiral-spiral configuration tethered to a slide via an Ab-bead. See text for interpretation.

These results differ from those with *E. coli* (13) and *Salmonella typhimurium* (20) in which flagellar reversal is not tightly coupled. Hopefully, the tethered-cell assay will be useful in interpreting the many motions of individual *Leptospira* cells undergoing a chemotactic stimulus and in understanding the nature of the mechanism which coordinates the shape of the cell ends.

ACKNOWLEDGMENTS

We appreciate the helpful discussions and suggestions of our colleagues, especially H. Berg, E. P. Greenberg, and D. Yelton. We thank R. Millecchia and M. Vance for computer assistance, and P. McCuskey for help with kine-recording.

This research was supported by Public Health Service grant DEO4645 from the National Institute of Dental Research.

LITERATURE CITED

1. **Berg, H. C.** 1976. Does the flagellar rotary motor step? Cold Spring Harbor Conf. Cell Proliferation. **3**:A47–A56.
2. **Berg, H. C., D. B. Bromley, and N. W. Charon.** 1978. Leptospiral motility, p. 285–294. *In* R. Y. Stanier, H. J. Rogers, and J. B. Ward (ed.), Relations between structure and function in the prokaryotic cell. 28th Symposium of the Society for General Microbiology. Cambridge University Press, Cambridge.
3. **Berg, H. C., and L. Turner.** 1979. Movement of microorganisms in viscous environments. Nature (London) **278**:349–351.
4. **Birch-Andersen, A., K. Hovind-Hougen, and C. Borg-Petersen.** 1973. Electron microscopy of *Leptospira*. 1. *Leptospira* strain *Pomona*. Acta. Pathol. Microbiol. Scand. Sect. B **81**:665–676.
5. **Bromley, D. B., and N. W. Charon.** 1979. Axial filament involvement in the motility of *Leptospira interrogans*. J. Bacteriol. **137**:1406–1412.
6. **Canale-Parola, E.** 1978. Motility and chemotaxis of spirochetes. Annu. Rev. Microbiol. **32**:69–99.
7. **Carleton, O., N. W. Charon, P. Allender, and S. O'Brien.** 1979. Helix handedness of *Leptospira interrogans* as determined by scanning electron microscopy. J. Bacteriol. **137**:1413–1416.
8. **Charon, N. W., C. W. Lawrence, and S. O'Brien.** 1981. Movement of antibody-coated latex beads attached to the spirochete *Leptospira interrogans*. Proc. Natl. Acad. Sci. U.S.A. **78**: 7166–7170.
9. **Cox, P. J., and G. I. Twigg.** 1974. Leptospiral motility. Nature (London) **250**:260–261.
10. **Goulbourne, E. A., Jr., and E. P. Greenberg.** 1981. Chemotaxis of *Spirochaeta aurantia*: involvement of membrane potential in chemosensory signal transduction. J. Bacteriol. **148**:837–844.
11. **Holt, S. C.** 1978. Anatomy and chemistry of spirochetes. Microbiol. Rev. **42**:114–160.
12. **Hovind-Hougen, K.** 1976. Determination by means of electron microscopy of morphological criteria of value for classification of some spirochetes, in particular treponemes. Acta. Pathol. Microbiol. Scand. Sect. B **255**(Suppl.):1–41.
13. **Ishihara, A., J. E. Segall, S. M. Block, and H. C. Berg.** 1983. Coordination of flagella on filamentous cells of *Escherichia coli*. J. Bacteriol. **155**:228–237.
14. **Jarosch, R.** 1967. Studien zur Bewegungsmechanik der Bakterien und Spirochaten des Hochmoores. Oesterr. Bot. Z. **114**:255–306.
15. **Johnson, R. C., and S. Faine.** 1984. *Leptospira*, p. 62–67. *In* N. R. Krieg and J. G. Holt (ed.), Bergey's manual of determinative bacteriology, 9th ed., vol. 1. The Williams & Wilkins Co., Baltimore.
16. **Johnson, R. C., and V. G. Harris.** 1967. Differentiation of pathogenic and saprophytic leptospires. I. Growth at low temperatures. J. Bacteriol. **94**:27–31.
17. **Kayser, A., and M. Adrian.** 1978. Les spirochetes: sens de l'enroulement. Ann. Microbiol. (Paris) **129A**:351–360.
18. **Krieg, N. R., J. P. Tomelty, and J. S. Wells, Jr.** 1967. Inhibition of flagellar coordination in *Spirillum volutans*. J. Bacteriol. **94**:1431–1436.
19. **Lapidus, I. R., and H. C. Berg.** 1982. Gliding motility of *Cytophaga* sp. strain U67. J. Bacteriol. **151**:384–398.

20. **Macnab, R. M., and D. P. Han.** 1983. Asynchronous switching of flagellar motors on a single bacterial cell. Cell **32**:109–117.
21. **Macnab, R. M., and D. E. Koshland.** 1974. Bacterial motility and chemotaxis: light-induced tumbling response and visualization of individual flagella. J. Mol. Biol. **84**:399–406.
22. **Manson, M. D., P. Tedesco, H. C. Berg, F. M. Harold, and C. van der Drift.** 1977. A protonmotive force drives bacterial flagella. Proc. Natl. Acad. Sci. U.S.A. **74**:3060–3064.
23. **McCuskey, R. S.** 1981. *In vivo* microscopy of internal organs. Prog. Clin. Biol. Res. **59B**:79–87.
24. **Metzner, P.** 1920. Die Bewegung und Reizbeantwortung der bipolar gegeisselten *Spirillen*. Jahrb. Wiss. Bot. **59**:325–412.
25. **Noguchi, H.** 1918. Morphological characteristics and nomenclature of *Leptospira* (Spirochaeta) *icterohaemorrhagiae* (Inada and Ido). J. Exp. Med. **27**:575–592.
26. **Paster, B. J., and E. Canale-Parola.** 1980. Involvement of periplasmic fibrils in motility of spirochetes. J. Bacteriol. **141**: 359–364.
27. **Pate, J. L., and L. E. Chang.** 1979. Evidence that gliding motility in prokaryotic cells is driven by rotary assemblies in the cell envelopes. Curr. Microbiol. **2**:59–64.
28. **Shioi, J.-I., S. Matsuura, and Y. Imae.** 1980. Quantitative measurements of proton motive force and motility in *Bacillus subtilis*. J. Bacteriol. **144**:891–897.
29. **Silverman, M. R., and M. I. Simon.** 1974. Flagellar rotation and the mechanism of bacterial motility. Nature (London) **249**:73–74.
30. **Singer, J. M., C. M. Plotz, and R. Goldberg.** 1965. The detection of antiglobulin factors utilizing pre-coated latex particles. Arthritis Rheum. **8**:194–202.
31. **Spudich, J. L., and D. E. Koshland, Jr.** 1979. Specific inactivator of flagellar reversal in *Salmonella typhimurium*. J. Bacteriol. **139**:442–447.
32. **Taylor, G.** 1952. The action of waving cylindrical tails in propelling microscopic organisms. Proc. R. Soc. London Ser. A **211**:225–239.
33. **Usui, S., and I. Amidror.** 1982. Digital low-pass differentiation for biological signal processing. IEEE Trans. Biomed. Eng. **29**:686–693.
34. **Yoshii, Z.** 1978. Studies on the spiral direction of the *Leptospira* cell body. Proc. Jpn. Acad. **54B**:200–205.